Letters in High Energy Physics
ISSN: 2632-2714
Volume 2024

Enhanced Image Denoising Using Color Wiener Filtering with Optimized Low-Rank Approximation

Mrs. Rashmi Dharwadkar[1,a)], Dr. Bahubali. K. Shiragapur[2,b)]

[1]Research Scholar, School of Computer Science, Engineering and Applications, DY Patil International University, Pune, Maharashtra,India-411033

[2] Director, School of Computer Science, Engineering and Applications, DY Patil International University, Pune, Maharashtra, India-411033

[a)] Corresponding author: rashmidharwadkar1@gmail.com

[b)] bahubali.shiragapur@dypiu.ac.in

Abstract

Sparse representation and low-rank approximation are popular for image denoising, but struggle with complex structures in heavily degraded images due to inadequate local descriptors and coefficient shrinkage rules. Hence, this research introduces a novel approach for image denoising using Color Wiener Filtering with Optimized Low-Rank Approximation. The proposed model integrates gamma correction for contrast enhancement with Color Wiener Filtering and Optimized Low-Rank Approximation to effectively remove noise from various images. Additionally, L0 smoothing is employed to address blurring effects while preserving image edges. The study evaluates the proposed model's performance using key parameters, including Mean Squared Error (MSE), Peak Signal-to-Noise Ratio (PSNR), and Structural Similarity Index (SSIM). Results indicate that the proposed model achieves an average MSE of 0.075, PSNR of 44.47 decibels (dB) and SSIM of 0.961. The suggested model is compared to other traditional state-of-the-art approaches to validate its performance, and it is found that in terms of PSNR and SSIM, the proposed model surpassed all other state-of-the-art methods. Overall, this research highlights the challenges addressed by the proposed model, its attained results, and its superiority compared to existing approaches, positioning it as a promising solution for image-denoising applications.

Keywords: Image denoising, Color Wiener Filtering, Optimized Low-Rank Approximation, Peak Signal-to-Noise Ratio, Gamma correction

1. Introduction

Data collection and transmission inherently contribute noises into acquired images due to defective electronics, natural temperature fluctuations, and outside interference [1-3]. One of the most important tools for restoring clean images from noisy data is image denoising [4]. Finding reliable and effective image-denoising methods that work in all kinds of real-world situations has been a constant struggle for researchers over the last 40 years [5-8]. Denoising algorithms can be categorized as spatial domain and transformed domain methods [9-11]. Within the first group, methods based on partial differential equations (PDE), along with methods that include spatially changing convolution and approaches that are based on nonlocal means, are considered [12-13]. In PDE-based approaches, it is common practice to use a total variation (TV) filter to eliminate noise while maintaining the integrity of edges [14]. Television, on the other hand, presumes that the underlying images are piecewise smooth, which is sometimes not possible for real images. This creates staircase effects that are not desirable and results in the loss of structural information [15].

1.1 Types of Filters for image denoising

Digital camera images are shrunk, cropped, and converted to grayscale before being used in various experiments. To improve the image quality and eliminate noise before restoration, the following pretreatment filtering methods can be utilized:

- **Mean Filter**

The mean filter enhances image pixel values by averaging grayscale values in the neighbourhood,

reducing pixel intensity variations. It's a simple, intuitive technique for image enhancement, commonly used for smoothing and blurring, offering ease of implementation and effective reduction of noise [16].

- **Median filter**

The median filtering approach is a nonlinear statistical method for removing noise from images. It keeps the image's essential information while replacing each pixel's original grayscale value with the median of nearby pixels' grayscale values. This filter reduces noise in an image without introducing blurring in edges [17].

- **Weiner filter**

The wiener filter technique uses a statistical approach to remove noise from each pixel in an image. It combines inverse screening and noise reduction in the most efficient way possible. It is the best filter for lowering the total MSE when it comes to noise smoothing. It attempts to construct an image by limiting the difference between the actual and estimated images by the MSE [18].

Recently, there has been a lot of interest in the transformed domain denoising algorithms based on wavelet transform, sparse representation, and deep learning [19]. However, because of the fixed wavelet basis, which always produces noticeable visual aberrations, these methods are unable to adaptively capture many structural aspects of actual images [20–22]. This problem is avoided by sparse representation-based techniques, which learn data adaptive bases for imagine denoising [23]. Typically, these techniques entail manually resolving a challenging optimization problem and adjusting parameters to achieve nearly ideal results [24]. Deep learning-based techniques use large training data sets to build picture models, which are subsequently used for image denoising. This overcomes the drawbacks of the model-based methods previously described [25]. These techniques can produce very accurate results with a relatively small processing power requirement. Nevertheless, when there are differences between training and test images, these approaches frequently result in a notable loss in denoising performance since they require a lot of training data [26–28].

In this research, a novel Color Wiener Filtering (WF) model is designed for the effective restoration of detailed image structures and enhanced denoising. An enhanced low-rank approximation (LRA) technique is employed to evaluate reference images. This research's primary contributions are:

- Proposed the shape-adaptive kernel function to create the optimum Color WF, which minimizes mean square error as a local image descriptor.
- The research utilizes constrained covariance matrix reduction to estimate the reference picture using optimized LRA.
- Gamma correction is used to enhance the contrast and overall appearance of the image.
- L0 smoothing is applied to the denoised image to address the blurry effect while preserving edges.

The structure of the paper is organized as follows: section 1 provides an overview on image denoising, section 2 discussed the previous work of various authors, section 3 discusses the research methodology of the paper, section 4 discusses the result that are obtained after the implementation of the research methodology, and finally a conclusion and future scope is discussed in section 5.

2. Literature review

This section discussed the previous research of various authors done in the section of image denoising and increasing the overall quality of the image.

Chen et al. (2024) [29] introduced an image-denoising algorithm based on a time-fractional diffusion equation for high-quality image restoration. Extensive experiments revealed its effectiveness in removing Gaussian noise while preserving crucial structural information. Their approach outperformed several state-of-the-art denoising algorithms, showcasing its potential for advanced image restoration tasks.

Ankita Gupta (2024) [30] proposed a hybrid preprocessing technique aimed at noise elimination and contrast enhancement in chlorophyll fluorescence (CHF) images. Utilizing the Block Matching-3D (BM3D) method with gamma correction yielded the optimum results, boasting a mean PSNR of 0.54 and a mean MSE of 0.07, effectively maximizing image quality and clarity.

Saini et al. (2023) [31] introduced an optimization technique for impulse noise removal in digital grey-scale images, showcasing remarkable efficacy even at noise levels up to 70%. Their Residual learning-based optimization filter not only effectively removed noise but also preserved edges and sharpness, enhancing image quality and fidelity.

Chen et al. (2023) [32] proposed a robust principal component analysis method integrating nonconvex LRA and total variational regularization for image denoising. Their approach effectively preserved edge structure, important features, and visual quality, demonstrating superior performance over existing methods in brightness smoothing and feature preservation.

Karthikram and Saravanan (2023) [33] created an innovative deep-learning method specifically designed for reducing noise in computed tomography (CT) images. This model exhibited exceptional performance in global structural similarity and PSNR metrics, even in scenarios with unknown or specific noise levels, without relying on higher-dose reference images.

Oliveira et al. (2023) [34] introduced the Nonlocal Convolutional Neural Network Denoiser (NL-CNND) for denoising noisy hyperspectral images. Their method surpassed existing techniques in terms of PSNR, SSIM, and Spectral Angle Mapper (SAM) metrics, addressing the challenge of noise corruption in hyperspectral imagery effectively.

Singh et al. (2022) [35] suggested a deep learning-based architecture that preserves tiny features in CT images while removing Gaussian additive white noise. Their strategy, which combined the method noise idea with CNN, produced results that were encouraging for medical imaging applications: an average PSNR of 25.82, an SSIM of 0.85, and a computing time of 2.8760.

Meng and Zhang et al. (2022) [36] introduced a CNN-based grey image denoising method designed for high noise level environments. Their symmetric and dilated convolutional residual network, coupled with leaky Rectified Linear Unit (ReLU) and ReLU dual functions, significantly improved denoising efficacy and productivity, offering a promising solution for noisy image restoration tasks.

Bo et al. (2021) [37] proposed a novel nonconvex smooth rank approximation model for hyperspectral image denoising, surpassing nuclear norm regularization methods. Their approach, employing Laplace function regularization for low-rank matrix approximation, demonstrated superior performance in simulated and real data experiments, establishing its effectiveness in hyperspectral image restoration.

Cheng et al. (2021) [38] introduced the Noise Basis-Net (NBNet), a novel framework for image denoising incorporating subspace attention (SSA). Their hybrid model, leveraging SSA for basis generation and subspace projection within NBNet, achieved remarkable results on the Smartphone Image Denoising Dataset (SIDD) dataset by attaining a mean PSNR of 39.75 and a mean SSIM of 0.969, showcasing its potential for real-world denoising applications.

Tran et al. (2020) [39] proposed a two-step model based on generative adversarial networks for enhancing deep network denoisers' performance. Their approach involved training a two-step model to estimate noise distribution over a large image collection, achieving significant improvements in denoising performance, with an average PSNR of 42.28 and SSIM of 0.9525 on the SIDD dataset.

Based on the literature review provided, there are several potential research gaps regarding the robustness and adaptability of these methods across diverse types and levels of noise. Existing approaches often struggle to effectively handle complex noise patterns, which are prevalent in real-world scenarios. Furthermore, many algorithms mentioned above are tailored to specific noise distributions or assume a fixed noise level, limiting their applicability in dynamic environments where noise characteristics can vary; also, the fixed wavelet basis limits adaptability to diverse image structures, leading to noticeable artefacts. Thus, there is a pressing need for innovative denoising techniques that can seamlessly adapt to various noise profiles and offer superior performance in challenging conditions, ultimately enhancing the quality and reliability of denoised images across different applications.

3. Research Methodology

In this section, the research methodology of this research is discussed in detail. Figure 1 shows the proposed architecture of the research methodology. The proposed methodology combines gamma

correction for contrast enhancement with Color WF and Optimized LRA for removing noise in various images. Additionally, L0 smoothing is employed to address blurring effects while preserving image edges. Initially, gamma correction enhances image contrast. Then, Color Wiener Filtering and Optimized Low-Rank Approximation (OLRA) jointly remove noise while preserving image details. Finally, L0 smoothing further refines the denoised image by selectively smoothing areas of low texture while preserving edges, resulting in an enhanced denoising approach that effectively tackles noise, preserves image details, and maintains sharp edges.

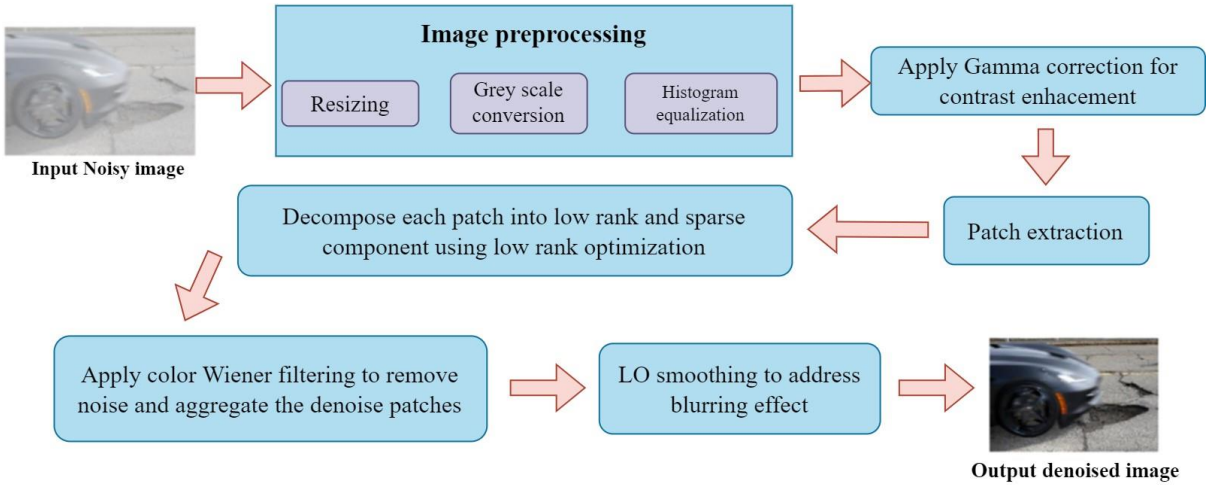

Figure 1. Proposed Architecture.

3.1 Dataset description

The dataset that is used in this research is an open-source dataset, which is known as the pothole detection dataset, which is easily available on the website of Kaggle. The 665 images in this dataset have bounding box annotations in PASCAL VOC format, which can be used to create detection models and serve as points of contact or points of view for road maintenance [40]. Figure 2 shows the types of images used in this research.

Figure 2. Dataset images.

3.2 Technique Used

The major techniques that are used in this research are discussed in detail description.

- **Color Wiener filtering model.**

Noise has a way of corrupting complex structures found in images, including edges, textures, and smooth areas. Unfortunately, current denoising techniques frequently fail to remove noise while recovering these intricate image structures. Among the several methods used to improve denoising performance, the second stage of BM3D employs conventional Wiener filtering (CWF) [41-42]. Nevertheless, it fails to efficiently construct complex image structures when combined with cutting-edge methods to remove noise. Hence, a new color WF model is proposed to reconstruct complex image structures accurately and enhance the denoising process. To depict local complicated image structures, this model uses a shape-aware color

function. In the given example, $y_i = C_i Y$ represents a patch in the noisy picture Y and $r_i = C_i R$ represents a patch in the reference image (R) at pixel i, where C_i is a matrix that extracts a patch from the image at pixel I [43-45]. Here is the formulated form of the suggested color WFM method:

$$\hat{X} = \left(\sum_i C'_i C_i\right)^{-1} \sum_i C'_i \left(\hat{h}_i * k_i o y_i / k_i\right) \quad (1)$$

In this context, $\hat{X}$ Represents the denoised image, which is seen as an estimate of the clean image X. C'_i is the transpose matrix of C_i. $\hat{h}_i$, with dimensions L × L, is the optimal color WF at pixel i. Finally, k_i is the shape-aware kernel function K at pixel i, which maps data from the signal space to its feature space [46]. To determine the optimum color WF $\hat{h}_i$ in Eq. (1), one follows these steps:

$$\hat{h}_i = \min E[e_i^2(j)], \quad \text{with } e_i = k_i \circ r_i - h_i * (k_i \circ y_i), \quad (2)$$

E depicts the expected value while $e_i(j)$ denotes the jth element of the patch error e_i.

- **Optimized low-rank approximation (OLRA)**

To begin developing the best KWF, it is essential to get a precise estimation of the reference image [47]. In this research, an OLRA approach is designed to determine the singular values in LRA with high precision. This approach incorporates structured sparsity and matrices of covariance and is based on restricted nuclear norm reduction [48-49]. Here is how OLRA calculates the patch group O_i in the reference picture R:

$$\widehat{O}_i = \min_{O_i} \|O_i O'_i\| \quad (3)$$

$$\text{s.t.} \quad \|G_i - O_i\|_F^2 < \varepsilon \quad (4)$$

A nuclear norm denoted as $\|.\| *$ reflects the group sparsity constraint, the Frobenius norm as $\|.\|_f$, and an error constraint as ξ.

3.3 Proposed algorithm

Step 1: Preprocessing

The input image is preprocessed to a fixed size of 512x512 pixels, converted to grayscale, and its contrast is enhanced using histogram equalization.

Step 2: Gamma Correction

Gamma correction is applied to the preprocessed grayscale image to further enhance its contrast.

Step 3: Patch Extraction

Placeholder for patch extraction. Typically, this step involves dividing the image into smaller overlapping patches for further processing, but it's not implemented in this code snippet.

Step 4: Low-Rank Approximation

Placeholder for LRA. No implementation is provided here.

Step 5: Optimization

Placeholder for optimization of the LRA.

Step 6: Color Wiener Filtering

Placeholder for color Wiener filtering.

Step 7: Patch Aggregation

An array **denoised_image** is initialized with the same dimensions as the pre-processed image. This array would typically be used to aggregate the denoised patches back into a single image.

Step 8: L0 Smoothing

L0 smoothing is applied to the denoised image using nonlocal means of denoising with L0 gradient minimization.

Step 9: Post-processing

Median blur with a kernel size of 3x3 is applied to the L0 smoothed image to further reduce noise and smooth out remaining artefacts.

Step 10: Return

The final post-processed image is returned as the result of the denoising and smoothing process.

End

4. Results and discussion

This section delves into the outcomes following the implementation of the proposed architecture. It begins with a discussion on evaluation metrics such as MSE, PSNR, and SSIM. The proposed model's performance is thoroughly evaluated based on these metrics. Finally, a comparative analysis with conventional approaches is conducted, primarily focusing on PSNR and SSIM metrics to gauge the efficacy and superiority of the proposed model in image denoising tasks.

4.1 Evaluation metrics

- **MSE –** The mean squared variance of the input and output pictures after reconstruction is what this metric measures. It's a standard way to measure how well algorithms can restore or rebuild images. For MSE, the formula is:

$$\mathrm{MSE} = \frac{1}{n \times m} \sum_{j=1}^{m} \left(l_{ij} - K_{ij}\right)^2 \quad (5)$$

The variables n and m represent the dimensions, specifically the height and width, of the images. The variable l_{ij} represents the intensity of the pixel located at position (i, j) in the first image. K_{ij} represents the brightness or strength of the pixel located at position (i, j) in the second image. A lower MSE signifies a greater resemblance between the images, as it suggests that the pixel counts are more closely aligned.

- **PSNR:** The PSNR is a statistic that is extensively utilized to evaluate the quality of a picture that has been reconstructed or compressed in comparison to the genuine unprocessed image. In decibels (dB), it is expressed, and the formula that is used to compute it is as follows:

$$\mathrm{PSNR} = 10 \log_{10} \left(\frac{\text{Max intensity of pixel}^2}{\mathrm{MSE}} \right) \quad (6)$$

- **SSIM**- A metric that is used to quantify the degree of resemblance between two images is called the SSIM. SSIM is determined by applying the formulas that are shown below:

$$\mathrm{SSIM}\,(x, y) = \frac{(2\mu_x \mu_y + c_1)(2\sigma_{xy} + c_2)}{(\mu_x^2 + \mu_y^2 + c_1)(\sigma_x^2 + \sigma_y^2 + c_2)} \quad (7)$$

Where x and y are compared image patches, μ_x and μ_y are the means of x and y, σ_x^2 and σ_y^2 are the variances of x and y. σ_{xy} is the covariance of x and y, c_1 and c_2 are small constants to stabilize the division.

4.2 Results analysis

Table 1 illustrates the performance evaluation of the proposed model, focusing on key parameters, including MSE, PSNR, and SSIM. The increment in noise levels from 10 to 40 correlates with a corresponding rise in MSE from 0.05 to 0.10. The average MSE achieved by the proposed model is recorded at 0.075. Conversely, PSNR values exhibit a decline from 46.78 to 42.25 as noise levels escalate, resulting in an average PSNR of 44.47. Similarly, the SSIM values decrease from 0.989 to 0.933 with increasing noise levels, averaging at 0.961.

These findings suggest that as noise levels intensify, the model's performance, as indicated by MSE, deteriorates. This degradation is further echoed in the diminishing PSNR and SSIM values, implying a reduction in image quality as noise increases. Figure 3 visually represents the performance trends of the proposed model, facilitating a clearer understanding of its efficacy under varying noise conditions.

Table 1 Performance evaluation of the proposed model

Parameters	**Noise level**			
	10	**20**	**30**	**40**
MSE	0.05	0.07	0.08	0.10
PSNR	46.78	44.82	44.05	42.24
SSIM	0.989	0.957	0.966	0.933

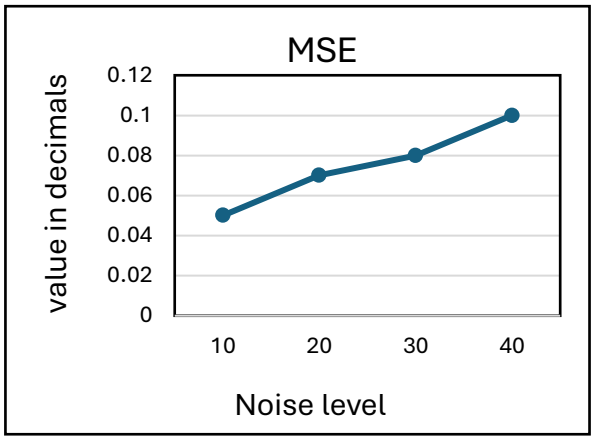

(a)

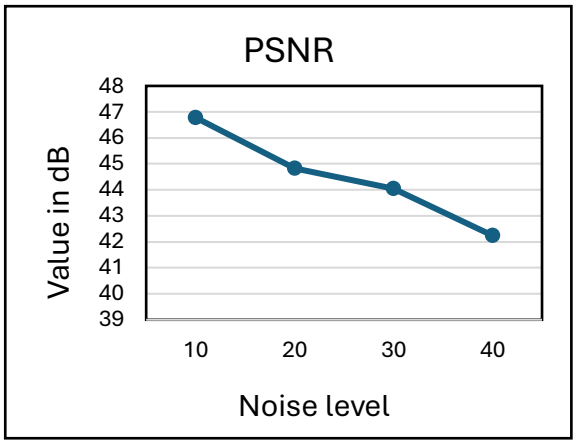

(b)

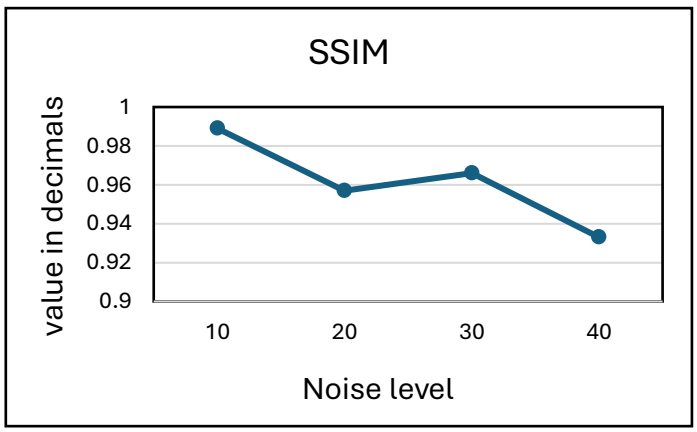

(c)

Figure 3 Performance graph of the proposed model on various parameters.

4.3 Comparative analysis

Table 2 provides a comparative analysis of various pothole detection models. Each model is listed by type CNN, NBNet, GAN, and Proposed model, along with the year of publication for the related research. The table also details the dataset used to train each model. The two key metrics used for comparison are Avg. PSNR and Avg. SSIM. Both metrics assess image quality, with higher values indicating better performance. Based on the obtained results, it is concluded that the proposed

model achieves the highest Avg. PSNR (44.47) and Avg. SSIM (0.961) compared to the other models. The proposed model appears to be the most effective for pothole detection based on these PSNR and SSIM metrics. Figure 4 visually represents the comparison of the proposed model with other conventional approaches in terms of PSNR and SSIM.

Table 2 Comparison of the proposed model with other conventional approaches

Model	Year	Dataset	Avg. PSNR	Avg. SSIM
CNN [35]	2022	CT images dataset	**25.82**	**0.85**
NBNet [38]	2021	SIDD	39.75	0.969
GAN [39]	2021	SIDD	42.28	0.9525
Proposed Model	2024	Pothole detection dataset	44.47	0.961

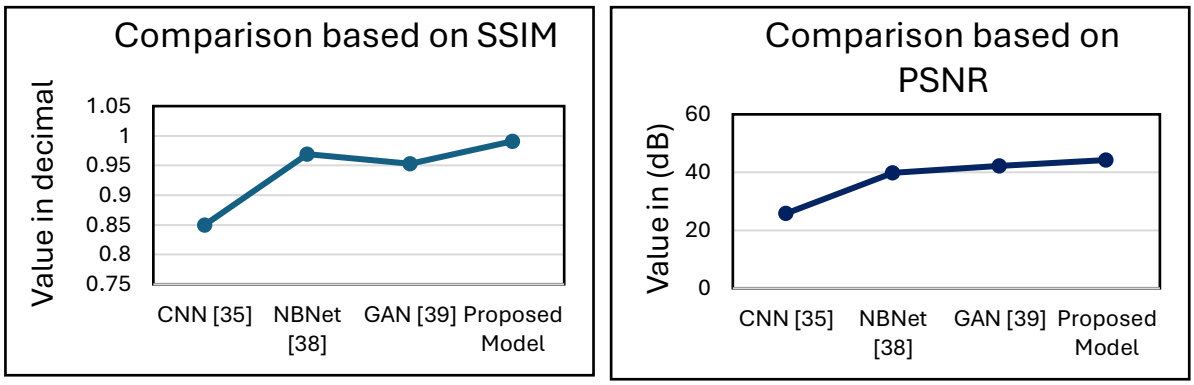

(a) (b)

Figure 4 Comparison Graph

5. Conclusion and future scope

The study presents a novel approach for image denoising through the integration of Color Wiener Filtering with Optimized Low-Rank Approximation, augmented by gamma correction and L0 smoothing techniques. On average, the suggested model achieves a 0.075 MSE, 44.47 dB PSNR, and 0.961 SSIM when tested against critical metrics. The suggested model outperforms the usual approaches, according to the comparative study, especially when considering PSNR and SSIM. The results illustrate how well the suggested method handles noise reduction while keeping the borders and features of the images intact. The study demonstrates that this model has great promise as an image-denoising solution and provides useful information for future improvements in image processing. Future studies could enhance image denoising by integrating advanced deep learning methods like CNNs to capture intricate image patterns. Additionally, exploring novel regularization techniques or optimization algorithms could enhance the efficiency and effectiveness of the denoising process.

References

1. Zhang, Yongqin, Ruiwen Kang, Xianlin Peng, Jun Wang, Jihua Zhu, Jinye Peng, and Hangfan Liu. "Image denoising via structure-constrained low-rank approximation." Neural Computing and Applications 32 (2020): 12575-12590.

2. Kalantari, Sadegh, Mehdi Ramezani, and Ali Madadi. "Introducing a New Hybrid Adaptive

Local Optimal Low-Rank Approximation Method for Denoising Images." International Journal of Industrial Electronics Control and Optimization 3, no. 2 (2020): 173-185.

3. Chen, Tianfei, Qinghua Xiang, Dongliang Zhao, and Lijun Sun. "An Unsupervised Image Denoising Method Using a Nonconvex Low-Rank Model with TV Regularization." Applied Sciences 13, no. 12 (2023): 7184.
4. Guo, Jing, Shuping Wang, Chen Luo, Qiyu Jin, and Michael Kwok-Po Ng. "Image Denoising by Gaussian Patch Mixture Model and Low-Rank Patches." arXiv preprint arXiv:2011.10290 (2020).
5. Wu, Xiaoce, Bingyin Zhou, Qingyun Ren, and Wei Guo. "Multispectral image denoising using sparse and graph Laplacian Tucker decomposition." Computational Visual Media 6 (2020): 319-331.
6. Lin, Jie, Ting-Zhu Huang, Xi-Le Zhao, Tian-Hui Ma, Tai-Xiang Jiang, and Yu-Bang Zheng. "A novel nonconvex low-rank tensor approximation model for hyperspectral image restoration." Applied Mathematics and Computation 408 (2021): 126342.
7. He, Chun, Ke Guo, and Huayue Chen. "An Improved Image Filtering Algorithm for Mixed Noise." Applied Sciences 11, no. 21 (2021): 10358.
8. Bo, Li, Luo Xuegang, and Lv Junrui. "Hyperspectral Image Denoising Based on Nonconvex Low-Rank Tensor Approximation and LP Norm Regularization." Mathematical Problems in Engineering 2021 (2021): 1-11.
9. Swamy, Somashekhar, and P. K. Kulkarni. "A basic overview on image denoising techniques." Int. Res. J. Eng. Technol. 7, no. 5 (2020): 850-857.
10. Oguzhanoglu, S., I. Kapucuoglu, and F. Sunar. "Comparison of Satellite Image Denoising Techniques in Spatial and Frequency Domains." The International Archives of the Photogrammetry, Remote Sensing and Spatial Information Sciences 43 (2022): 1241-1247.
11. Kong, Zhaoming, Xiaowei Yang, and Lifang He. "A comprehensive comparison of multi-dimensional image denoising methods." arXiv preprint arXiv:2011.03462 (2020).
12. Salamat, Nadeem, Malik Muhammad Saad Missen, and V. B. Surya Prasath. "Recent developments in computational color image denoising with PDEs to deep learning: a review." Artificial Intelligence Review (2021): 1-32.
13. Goyal, Bhawna, Ayush Dogra, Sunil Agrawal, Balwinder Singh Sohi, and Apoorav Sharma. "Image denoising review: From classical to state-of-the-art approaches." Information fusion 55 (2020): 220-244.
14. Li, Shuaihao, Bin Zhang, Xinfeng Yang, and Weiping Zhu. "Edge-guided second-order total generalized variation for Gaussian noise removal from the depth map." Scientific Reports 10, no. 1 (2020): 16329.
15. Wang, Junpu, Guili Xu, Chunlei Li, Zhengsheng Wang, and Fuju Yan. "Surface defects detection using nonconvex total variation regularized RPCA with kernelization." IEEE Transactions on Instrumentation and Measurement 70 (2021): 1-13.
16. Shah, Anwar, Javed Iqbal Bangash, Abdul Waheed Khan, Imran Ahmed, Abdullah Khan, Asfandyar Khan, and Arshad Khan. "Comparative analysis of median filter and its variants for removal of impulse noise from gray scale images." Journal of King Saud University-Computer and Information Sciences 34, no. 3 (2022): 505-519.
17. Christo, Mary Subaja, K. Vasanth, and R. Varatharajan. "A decision-based asymmetrically trimmed modified winsorized median filter for the removal of salt and pepper noise in images and videos." Multimedia Tools and Applications 79, no. 1 (2020): 415-432.
18. Dogariu, Laura-Maria, Jacob Benesty, Constantin Paleologu, and Silviu Ciochină. "An insightful overview of the Wiener filter for system identification." Applied Sciences 11, no. 17 (2021): 7774.
19. Mishro, Pranaba K., Sanjay Agrawal, Rutuparna Panda, and Ajith Abraham. "A survey on state-of-the-art denoising techniques

for brain magnetic resonance images." IEEE Reviews in Biomedical Engineering 15 (2021): 184-199.

20. Wang, Zhisen, Zhuoyi Li, Xuanxuan Teng, and Deshan Chen. "LPMsDE: Multi-Scale Denoising and Enhancement Method Based on Laplacian Pyramid Framework for Forward-Looking Sonar Image." IEEE Access 11 (2023): 132942-132954.
21. Zhang, Ying. "Nonlocal clustering via sparse prior for sports image denoising." EAI Endorsed Transactions on Scalable Information Systems 9, no. 4 (2022): e14-e14.
22. Wosiak, Agnieszka, and Aleksandra Dura. "Hybrid method of automated EEG signals' selection using reversed correlation algorithm for improved classification of emotions." Sensors 20, no. 24 (2020): 7083.
23. Dutta, Sayantan. "Novel Prospects of Image Restoration Inspired by Concepts of Quantum Mechanics." PhD diss., Université Paul Sabatier-Toulouse III, 2023.
24. Liu, Sixin, Yuhan Chen, Chaopeng Luo, Hejun Jiang, Hong Li, Hongqing Li, and Qi Lu. "Particle Swarm Optimization-Based Variational Mode Decomposition for Ground Penetrating Radar Data Denoising." Remote Sensing 14, no. 13 (2022): 2973.
25. El-Shafai, Walid, Samy Abd El-Nabi, El-Sayed M. El-Rabaie, Anas M. Ali, Naglaa F. Soliman, Abeer D. Algarni, Abd El-Samie, and E. Fathi. "Efficient Deep-Learning-Based Autoencoder Denoising Approach for Medical Image Diagnosis." Computers, Materials & Continua 70, no. 3 (2022).
26. Izadi, Saeed, Darren Sutton, and Ghassan Hamarneh. "Image denoising in the deep learning era." Artificial Intelligence Review 56, no. 7 (2023): 5929-5974.
27. He, Yuru, Shuangliang Cao, Hongyan Zhang, Hao Sun, Fanghu Wang, Huobiao Zhu, Wenbing Lv, and Lijun Lu. "Dynamic PET image denoising with deep learning-based joint filtering." IEEE Access 9 (2021): 41998-42012.
28. Pang, Tongyao, Huan Zheng, Yuhui Quan, and Hui Ji. "Recorrupted-to-recorrupted: Unsupervised deep learning for image denoising." In Proceedings of the IEEE/CVF conference on computer vision and pattern recognition, pp. 2043-2052. 2021.
29. Chen, Huaiguang, Haili Qiao, Wenyu Wei, and Jin Li. "Time fractional diffusion equation based on Caputo fractional derivative for image denoising." Optics & Laser Technology 168 (2024): 109855.
30. Gupta, Ankita. "Improved Hybrid Preprocessing Technique for Effective Segmentation of Wheat Canopies in Chlorophyll Fluorescence Images." EAI Endorsed Transactions on AI and Robotics 3 (2024).
31. Saini, Ashish, Nasib Singh Gill, and Preeti Gulia. "Grayscale image denoising technique using regression-based residual learning." Multimedia Tools and Applications 83, no. 2 (2024): 3547-3566.
32. Chen, Tianfei, Qinghua Xiang, Dongliang Zhao, and Lijun Sun. "An Unsupervised Image Denoising Method Using a Nonconvex Low-Rank Model with TV Regularization." Applied Sciences 13, no. 12 (2023): 7184.
33. KARTHIKRAM, A., and M. SARAVANAN. "LOCALIZED NETWORK MODEL FOR IMAGE DENOISING AND PREDICTION USING LEARNING APPROACHES." Journal of Theoretical and Applied Information Technology 101, no. 20 (2023).
34. De Oliveira, Gabriel A., Larissa M. Almeida, Eduardo R. De Lima, and Luís Geraldo P. Meloni. "Deep Convolutional Network Aided by Nonlocal Method for Hyperspectral Image Denoising." IEEE Access (2023).
35. Singh, Abhishek, Manoj Diwakar, Reena Gupta, Sarvesh Kumar, Alakananda Chakraborty, Eshan Bajal, Muskan Jindal et al. "A Method Noise-Based Convolutional Neural Network Technique for CT Image Denoising." Electronics 11, no. 21 (2022): 3535.
36. Meng, Yizhen, and Jun Zhang. "A Novel Gray Image Denoising Method Using Convolutional

Neural Network." IEEE Access 10 (2022): 49657-49676.

37. Bo, Li, Luo Xuegang, and Lv Junrui. "Hyperspectral Image Denoising Based on Nonconvex Low-Rank Tensor Approximation and lp Norm Regularization." Mathematical Problems in Engineering 2021 (2021): 1-11.
38. Cheng, Shen, Yuzhi Wang, Haibin Huang, Donghao Liu, Haoqiang Fan, and Shuaicheng Liu. "Nbnet: Noise basis learning for image denoising with subspace projection." In Proceedings of the IEEE/CVF conference on computer vision and pattern recognition, pp. 4896-4906. 2021.
39. Tran, Linh Duy, Son Minh Nguyen, and Masayuki Arai. "GAN-based noise model for denoising real images." In Proceedings of the Asian Conference on Computer Vision. 2020.
40. https://www.kaggle.com/datasets/andrewmvd/pothole-detection?resource=download.
41. Gu, Shuhang, Qi Xie, Deyu Meng, Wangmeng Zuo, Xiangchu Feng, and Lei Zhang. "Weighted nuclear norm minimization and its applications to low-level vision." International journal of computer vision 121 (2017): 183-208.
42. Mbarki, Zouhair, Hassene Seddik, and Ezzedine Ben Braiek. "Non-blind image restoration scheme combining parametric Wiener filtering and BM3D denoising technique." In 2018 4th International Conference on Advanced Technologies for Signal and Image Processing (ATSIP), pp. 1-5. IEEE, 2018.
43. Kalyani, N., Tirunelveli Levengipuram, and A. Velayudham. "Novel framework using BM3D with Hard thresholding and Wiener filters for Image denoising." International Journal of Applied Engineering Research 10, no. 22: 2015.
44. Zhang, Yongqin, Jinsheng Xiao, Jinye Peng, Yu Ding, Jiaying Liu, Zongming Guo, and Xiaopeng Zong. "Kernel Wiener filtering model with a low-rank approximation for image denoising." Information Sciences 462 (2018): 402-416.
45. Ramadan, Zayed M. "Effect of kernel size on Wiener and Gaussian image filtering." TELKOMNIKA (Telecommunication Computing Electronics and Control) 17, no. 3 (2019): 1455-1460.
46. Ahmed, Zouhour Ben, and Nabil Derbel. "Identification of Parallel-Cascade Wiener System using Tensor Decomposition of an associated Volterra kernel." International Journal of Mathematical Models and Methods in Applied Sciences 16 (2022): 140-145.
47. Peng, Jiangtao, Weiwei Sun, Heng-Chao Li, Wei Li, Xiangchao Meng, Chiru Ge, and Qian Du. "Low-rank and sparse representation for hyperspectral image processing: A review." IEEE Geoscience and Remote Sensing Magazine 10, no. 1 (2021): 10-43.
48. Chen, Yong, Ting-Zhu Huang, Wei He, Xi-Le Zhao, Hongyan Zhang, and Jinshan Zeng. "Hyperspectral image denoising using factor group sparsity-regularized nonconvex low-rank approximation." IEEE Transactions on Geoscience and Remote Sensing 60 (2021): 1-16.
49. Qiu, Xiaoqun, Zhen Chen, Saifullah Adnan, and Hongwei He. "Improved MR image denoising via low-rank approximation and Laplacian-of-Gaussian edge detector." IET Image Processing 14, no. 12 (2020): 2791-2798.